

COMMUNICATION

Development of a Fluoride-anion Sensor based on Aggregation of a Dye-Modified Polyhedral Oligomeric Silsesquioxane

Daisuke Iizuka, Masayuki Gon, Kazuo Tanaka* and Yoshiki Chujo

Received 00th January 20xx,
Accepted 00th January 20xx

DOI: 10.1039/x0xx00000x

We report a new concept for the turn-on fluoride sensor based on aggregation of dye-modified polyhedral oligomeric silsesquioxane (POSS). The dye-modified POSS aggregation initially shows weak fluorescence, while intense fluorescence can be obtained when fluoride breaks POSS cores following the dye releasing.

Fluoride anions play various important roles in our daily lives, such as in drinking water and toothpaste owing to their beneficial effects on dental health. However, since fluoride deficiency or overconsumption is known to have adverse effects on the human body, as the U.S. Department of Health and Human Services recommends that fluoride levels in drinking water from 0.7 to 1.2 ppm are appropriate, there is still a great demand for developing chemical sensors that can detect fluoride anions with high sensitivity.¹ The electrochemical approach is the most well-established method with high sensitivity, whereas delicate instrumentation and time-consuming manipulations are necessary.² ¹⁹F NMR spectroscopy is also effective, while the detection limit is only at the micromolar level. Considering this, detection of fluoride anions by fluorescence is an approach that has attracted much attention because of its ease of handling and high sensitivity.³ Fluoride-selective optical sensors can be achieved by utilizing the reaction between fluoride and Lewis acid^{4–6}, especially Si atom.^{3,7–11} Meanwhile such sensors have excellent anion selectivity, their molecular designs are generally complicated.

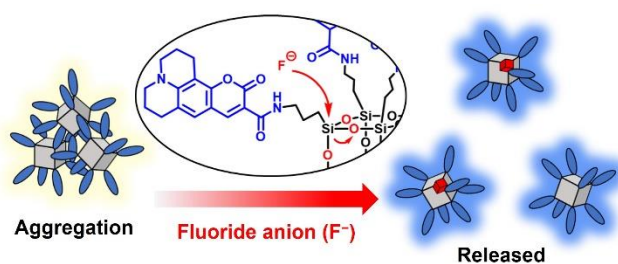
Polyhedral oligomeric silsesquioxane (POSS) derivatives which are composed of Si–O core and flexible organic side chains have been attracted attention as organic-inorganic hybrids.^{12–14} Among them, cubic T8 POSS (hereafter referred to as POSS for simplicity) is a skeleton that has been widely studied because of designability of functions.^{15–17} We called a series of POSS derivatives as designable hybrid materials based on the

concept of “element-blocks”, which are functional units composed of various groups of elements, to create advanced materials.^{17–20} As POSS molecules are containing silicon atoms, they exhibit unique affinity to fluoride anions and their function has been widely studied such as fluoride encapsulation^{21–24} and the rearrangement reaction.^{25,26} POSS derivatives have been also incorporated in several fluoride sensors for their chemical and thermal stability and versatile molecular designs towards various detection modes such as turn-on²⁷ and turn-off responses^{28,29} and color changes^{30–34}. In these studies, decomposition of the POSS nanocage by fluoride anions is a key step. Therefore, to completely proceed POSS degradation followed by the detection, excess amount of fluoride anions is essential. Hence, there is limitation to improve sensitivity based on conventional sensing strategies. Meanwhile, Some POSS derivatives are known to form stable nano- to micro-ordered aggregates in solution without precipitation.^{32,35–37} This is probably because such POSS derivatives could agglomerate with each other by the strong hydrophobic effect^{38–40} but cannot aggregate beyond a certain size due to the bulkiness of their side chains at each vertex. Although such behaviours of POSS are very attractive, few studies have intentionally utilized this property for a certain application.

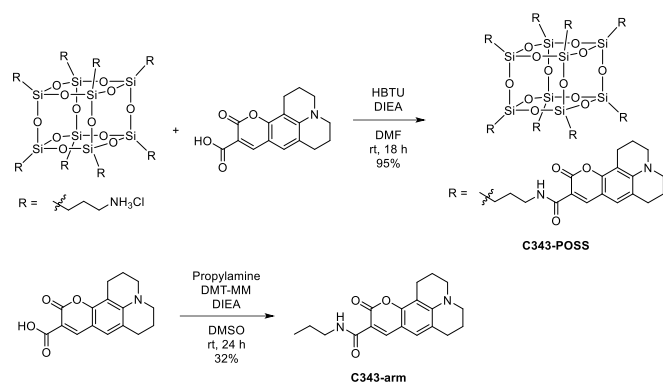
Herein, we report the novel fluoride sensor based on eight coumarin dyes-modified POSS (Scheme 1). As we presumed, the dye-modified POSS can form less fluorescent stable aggregation in THF/CHCl₃ mixed solutions. By adding fluoride anions, the reaction with one of POSS molecules followed by the partial collapse of the silica cage was induced. Subsequently, aggregation was released, and emission enhancement can be observed. On the basis of this mechanism, the turn-on response upon addition of fluoride anions can be observed with good sensitivity, selectivity and anti-interference ability. The dynamic light scattering (DLS) measurement, mass spectrometry and ¹⁹F NMR spectroscopy revealed that the emission enhancement should be triggered by Si–O bonds cleavage accompanied with exposure of hydrophilic anion (Si–O[–]) leading to release of dye-modified POSS from aggregates in the initial step followed by

^a Department of Polymer Chemistry, Graduate School of Engineering, Kyoto University Katsura, Nishikyo-ku, Kyoto 615-8510, Japan Address here.

[†] POSS[®] is an active registered trademark of Hybrid Plastics, Inc. Electronic Supplementary Information (ESI) available: [details of any supplementary information available should be included here]. See DOI: 10.1039/x0xx00000x



Scheme 1. Presumed mechanism of the fluoride anion sensor based on eight coumarin dyes-modified POSS.



Scheme 2. Synthetic route to **C343-POSS** and chemical structure of **C343-arm**.

ejection of coumarin dyes. By applying the reactivity of POSS with fluoride anions for switching from aggregation to dispersion states, sensitive detection can be realized.

Scheme 2 shows the synthetic route for **C343-POSS**. We chose coumarin C343 as a dye molecule because it was susceptible to concentration quenching when accumulated in the POSS scaffold due to intermolecular interactions. **C343-POSS** was synthesized by a condensation reaction with octakis(3-aminopropyl) POSS hydrochloride (**Amino-POSS**) and C343 in 95% isolated yield. The completely eight-substituted POSS was precipitated and collected simply by filtration. Figure S1 shows the ¹H NMR spectrum of **C343-POSS**. From the integration ratio of the signal peak from the triplet amide proton (8.81 ppm), it was confirmed that eight C343 units can be covalently attached to the POSS moiety. The signal at -66.9 ppm in the ²⁹Si NMR spectrum indicates that the cubic T8 POSS cage should remain intact (Figure S3). To compare the photophysical properties, we also synthesized the model compound **C343-arm**, which corresponds to one side chain of **C343-POSS**. These structures were also confirmed by ¹³C NMR spectroscopy (Figures S2 and S5), a high-resolution mass spectrometry, an elemental analysis and FT-IR spectra (Figure S6).

The photophysical properties of **C343-POSS** and **C343-arm** were measured in CHCl₃ (Table S1). Figures 1a and 1b present the absorption and emission spectra of **C343-POSS** and **C343-arm**, respectively. Both absorption spectra exhibited similar shapes, while the molar extinction coefficient (ϵ) per C343 unit of **C343-POSS** was smaller than that of **C343-arm**. The emission spectra showed that both **C343-POSS** and **C343-arm** had the

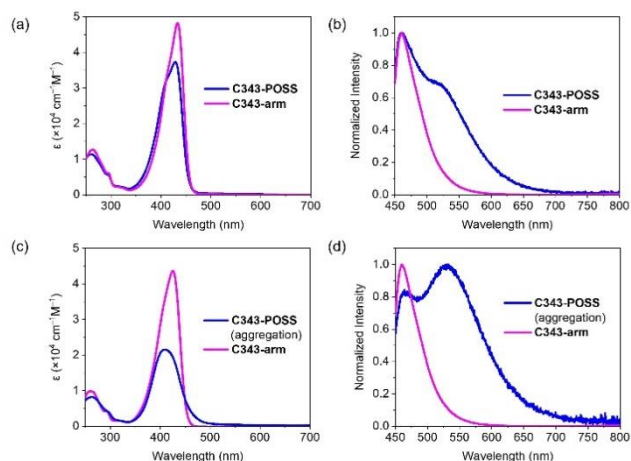


Figure 1. (a) Absorption (1.6×10^{-5} M per C343 unit) and (b) emission spectra (8.0×10^{-6} M per C343 unit) of **C343-POSS** and **C343-arm** in CHCl₃ solution. (c) Absorption and (d) emission spectra of **C343-POSS** and **C343-arm** in THF/CHCl₃ (99/1 v/v) mixed solution (1.6×10^{-5} M for C343 unit).

emission band with the peak (λ_{em}) around 460 nm, while **C343-POSS** had another much longer emission band, which was attributed to the excimer emission and dominantly observed in solid (Figure S7). Moreover, **C343-POSS** exhibited a significant decrease in absolute fluorescence quantum yield ($\Phi_{PL} = 30\%$) compared to **C343-arm** ($\Phi_{PL} = 85\%$). These results indicate that C343 moieties strongly interact with each other when accumulated in POSS. We next investigated the photophysical properties in their aggregation state in THF as a poor solvent. From the DLS measurements, it was shown that **C343-POSS** expectedly had a number-weighted hydrodynamic size of 78.8 ± 15.3 nm (Figure S8) with optical transparency in the THF/CHCl₃ (99/1 v/v, 1.6×10^{-5} M per C343 unit) solution. Figures 1c and 1d show the absorption and emission spectra of **C343-POSS** and **C343-arm** in this solution, respectively. Compared with the CHCl₃ solution, ϵ per the C343 unit of **C343-POSS** significantly decreased and the baseline was slightly elevated, suggesting the existence of aggregation formation. The emission from **C343-POSS** was weak ($\Phi_{PL} = 9\%$) and dominated by excimer emission. These results indicated that **C343-POSS** aggregation in the THF/CHCl₃ mixed solution should be suitable for constructing the turn-on fluoride detection system.

The fluoride sensing ability was investigated using the THF/CHCl₃ (99/1 v/v) mixed solution. As a result of solvent optimization, THF was found to be the most effective solvent for the fluoride detection (Figure S9). Upon the addition of tetrabutylammonium fluoride (TBAF) in THF as the fluoride anion source, the enhancement of monomer emission accompanied by fluorescence color change was observed (Figure 2a). According to the IUPAC equation,⁴¹ the limit of detection was determined to be $0.70 \mu\text{M}$ (Figure S10). Anion selectivity was then evaluated using various tetrabutylammonium salts (Figure 2b). Different from the fluoride anion, significant emission enhancement was not discerned upon the addition of other anions, meaning that

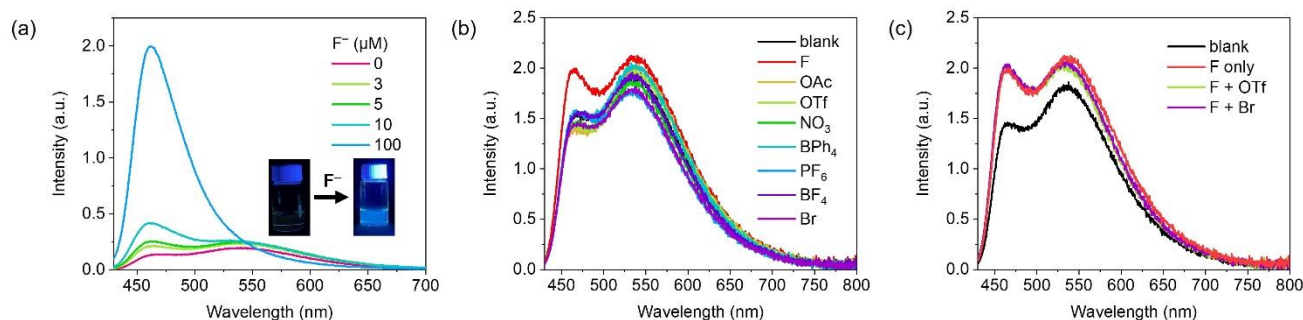


Figure 2. (a) Fluorescence enhancement upon addition of F^- . (b) Emission spectra upon addition of other anions (1.0×10^{-5} M). (c) Emission spectra upon addition of F^- and other anions (1.0×10^{-5} M for each). **[C343-POSS]** = 1.6×10^{-5} M per C343 unit in THF/ $CHCl_3$ (9/1 v/v) mixed solution. The cation is tetrabutylammonium (TBA). Detail sample preparation methods are shown in Supporting Information.

the sensor has excellent anion selectivity. Moreover, detection of fluoride anions was available even when other anions were coexisting (Figure 2c).

To clarify the sensing mechanism of **C343-POSS** aggregation towards fluoride ions, we conducted DLS measurements, mass spectrometry and ^{19}F NMR spectroscopy. **C343-POSS** aggregation in the THF/ $CHCl_3$ (9/1 v/v) mixed solution has a hydrodynamic size of 989.1 ± 214.2 nm after incubation at room temperature for 12 h (Figure 3a, blue). Upon the addition of 3 equiv. of TBAF to the **C343-POSS** aggregates, a significant decrease in particle size was observed (Figure 3a, red). It was also confirmed that the particle size remained unchanged after 7 h of standstill. Furthermore, when an excess amount of TBAF was added to the solution, aggregation was hardly observed. When the solution was examined by mass spectrometry, several decomposition products based on the reaction of silicon and fluoride were detected (Figures 3b and S11). The decomposition product containing one fluoride was not confirmed, suggesting that the reaction of silicon and fluoride anions triggers the POSS collapse, leading to the solubilization of C343 moieties and emission enhancement.

Figure 3c shows ^{19}F NMR spectra before and after the addition of TBAF (10 equiv.) to the **C343-POSS** solution in $CDCl_3$. The appearance of the new peak at -117 ppm indicated Si-F bond formation according to the reports on POSS-based fluoride sensors.^{30,32} From the chemical shift of compounds reported in previous studies (Table S2),^{42,43} the chemical structure of this new peak was expected to be the decomposition product **D1**. Although generation of **D1** requires multiple fluoride anions, the fluorescent enhancement induced by release of aggregation can be observed even in $3 \mu M$ of TBAF (1.5 equiv.) (Figure 2a). Other peaks were degradation products of TBAF because they were also found when TBAF in $CDCl_3$ was left at room temperature for 12 h (Figure S12). Moreover, in ^{29}Si NMR spectra, slightly shifted peak as well as the new peak were observed after addition of TBAF, and they should be originated from **C343-POSS** and damaged POSS (Figure S13).

It has been known that fluoride sensors can be also designed to use hydrogen bonding for the target recognition.^{44,45} For instance, a design in which fluoride is inserted between the two amide bonds to induce the excimer emission of fluorophores

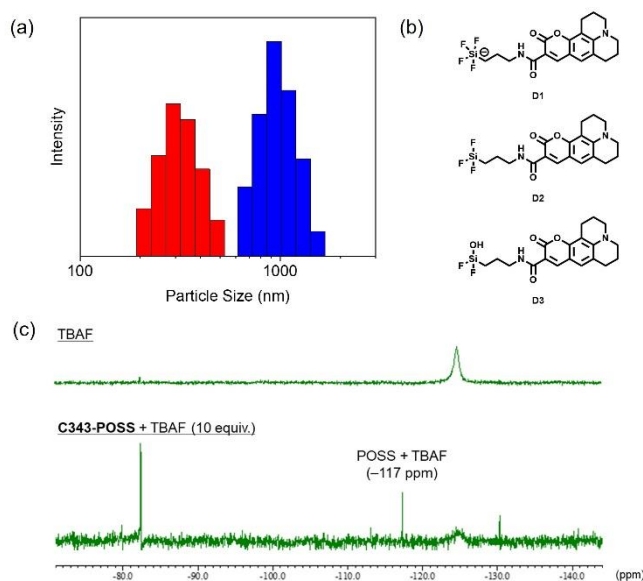


Figure 3. (a) Number-averaged hydrodynamic size distribution of **C343-POSS** (8.0×10^{-5} M per C343 unit) in THF/ $CHCl_3$ (9/1 v/v) mixed solution before (blue) and after (red) the addition of 3 equiv. of TBAF. (b) Chemical structures of the dyes found by mass spectrometry after the reaction of **C343-POSS** and TBAF (15 equiv.). (c) ^{19}F NMR spectra of TBAF and **C343-POSS** + TBAF (10 equiv.) in $CDCl_3$.

has also been reported.⁴⁴ Based on these examples, it is possible that such an insertion also occurs in our **C343-POSS**, and therefore we investigated this contribution by 1H NMR. When 4 equiv. of TBAF were added to **C343-POSS** in $CDCl_3$, critical changes were hardly observed in the 1H NMR spectrum (Figure S14), whereas significant signal shifts of the amide proton were observed in previous studies.⁴⁴ These data indicate that fluoride insertion to **C343-POSS**, which can lower the fluoride sensitivity, should be negligible in our system.

The accumulation of coumarin dyes with POSS can be expected to improve thermal stability. The decomposition temperatures (T_{d5}) of **C343-POSS** and **C343-arm** were measured by thermogravimetric analysis (TGA) in N_2 atmosphere (Figure

S15). The T_d of **C343-POSS** is 361 °C, which is very much higher than that of **C343-arm** (284 °C). A differential scanning calorimetry (DSC) study was also conducted (Figure S16). The glass transition temperature (T_g) and melting point (T_m) of **C343-arm** were determined as 26 and 169 °C, respectively, while significant peaks were not observed from **C343-POSS**. After the 1st heat cycle with **C343-POSS**, crystallization was not observed during cooling and heating cycles, suggesting the formation of amorphous state in the case of **C343-POSS**. These results clearly indicate that POSS connection plays an important role in enhancing thermal stability.

In conclusion, we have developed the turn-on fluoride sensor with a new conceptual approach based on POSS aggregation. The fluorescent sensor displayed good sensitivity, selectivity and anti-interference ability for the fluoride detection. To our knowledge, this is the first report of the turn-on fluoride sensor with the signal amplification system based on the switching from aggregation to dispersion triggered by the chemical reactions. Our new concept paves a new way for developing turn-on fluoride sensors. In this study, we demonstrate the sensing system only in organic solvents. Since water-dispersibility can be improved by decreasing the number of dye molecules around POSS, it is presumable that fluoride anions in aqueous media might be detectable with these next generation of hydrophilic POSS molecules based on the same strategy.

This work was partially supported by the SEI Group CSR Foundation (for M.G.), JSPS KAKENHI Grant Numbers JP21H02001 and JP21K19002 (for K.T) and JP17H01220 and JP P24102013 (Y.C.)

Conflicts of interest

There are no conflicts to declare.

Notes and references

- 1 S. Peckham and N. Awofeso, *Sci. World J.*, 2014, **2014**, 1–10.
- 2 C. Bresner, S. Aldridge, I. A. Fallis, C. Jones and L.-L. Ooi, *Angew. Chem. Int. Ed.*, 2005, **44**, 3606–3609.
- 3 Y. Zhou, J. F. Zhang and J. Yoon, *Chem. Rev.*, 2014, **114**, 5511–5571.
- 4 I.-S. Ke, M. Myahkostupov, F. N. Castellano and F. P. Gabbai, *J. Am. Chem. Soc.*, 2012, **134**, 15309–15311.
- 5 M. Miyata and Y. Chujo, *Polym. J.*, 2002, **34**, 967–969.
- 6 C. R. Wade, A. E. J. Broomsgrove, S. Aldridge and F. P. Gabbai, *Chem. Rev.*, 2010, **110**, 3958–3984.
- 7 X.-F. Yang, H. Qi, L. Wang, Z. Su and G. Wang, *Talanta*, 2009, **80**, 92–97.
- 8 Y. Peng, Y.-M. Dong, M. Dong and Y.-W. Wang, *J. Org. Chem.*, 2012, **77**, 9072–9080.
- 9 S. Y. Kim and J.-I. Hong, *Org. Lett.*, 2007, **9**, 3109–3112.
- 10 R. Hu, J. Feng, D. Hu, S. Wang, S. Li, Y. Li and G. Yang, *Angew. Chem. Int. Ed.*, 2010, **49**, 4915–4918.
- 11 T.-H. Kim and T. M. Swager, *Angew. Chem. Int. Ed.*, 2003, **42**, 4803–4806.
- 12 H. Zhou, Q. Ye and J. Xu, *Mater. Chem. Front.*, 2017, **1**, 212–230.
- 13 R. Y. Kannan, H. J. Salacinski, P. E. Butler and A. M. Seifalian, *Acc. Chem. Res.*, 2005, **38**, 879–884.
- 14 Y. Du and H. Liu, *Dalton. Trans.*, 2020, **49**, 5396–5405.
- 15 K. Tanaka and Y. Chujo, *J. Mater. Chem.*, 2012, **22**, 1733–1746.
- 16 A. Fina, O. Monticelli and G. Camino, *J. Mater. Chem.*, 2010, **20**, 9297.
- 17 M. Gon, K. Tanaka and Y. Chujo, *Chem. Asian J.*, 2022, **17**, e202200144.
- 18 M. Gon, K. Tanaka and Y. Chujo, *Polym. J.*, 2018, **50**, 109–126.
- 19 Y. Chujo and K. Tanaka, *Bull. Chem. Soc. Jpn.*, 2015, **88**, 633–643.
- 20 K. Tanaka and Y. Chujo, *Polym. J.*, 2020, **52**, 555–566.
- 21 A. R. Bassindale, M. Pourny, P. G. Taylor, M. B. Hursthouse and M. E. Light, *Angew. Chem. Int. Ed.*, 2003, **42**, 3488–3490.
- 22 S. E. Anderson, D. J. Bodzin, T. S. Haddad, J. A. Boatz, J. M. Mabry, C. Mitchell and M. T. Bowers, *Chem. Mater.*, 2008, **20**, 4299–4309.
- 23 M. Laird, P. Gaveau, P. Trens, C. Carcel, M. Unno, J. R. Bartlett and M. Wong Chi Man, *New J. Chem.*, 2021, **45**, 4227–4235.
- 24 M. Laird, C. Totée, P. Gaveau, G. Silly, A. Van der Lee, C. Carcel, M. Unno, J. R. Bartlett and M. Wong Chi Man, *Dalton. Trans.*, 2021, **50**, 81–89.
- 25 M. Z. Asuncion and R. M. Laine, *J. Am. Chem. Soc.*, 2010, **132**, 3723–3736.
- 26 J. C. Furgal, T. Goodson III and R. M. Laine, *Dalton. Trans.*, 2016, **45**, 1025–1039.
- 27 Y.-T. Zeng, S.-Y. Gao, K. Traskovskis, B. Gao and X.-K. Ren, *Dyes Pigm.*, 2021, **193**, 109491.
- 28 F. Du, Y. Bao, B. Liu, J. Tian, Q. Li and R. Bai, *Chem. Commun.*, 2013, **49**, 4631.
- 29 P. Siripanich, T. Bureerug, S. Channungkalakul, M. Sukwattanasinitt and V. Ervithayasuporn, *Organometallics*, 2022, **41**, 201–210.
- 30 H.-J. Ben, X.-K. Ren, B. Song, X. Li, Y. Feng, W. Jiang, E.-Q. Chen, Z. Wang and S. Jiang, *J. Mater. Chem. C*, 2017, **5**, 2566–2576.
- 31 S. Channungkalakul, V. Ervithayasuporn, S. Hanpravit, M. Masik, N. Prigyai and S. Kiatkamjornwong, *Chem. Commun.*, 2017, **53**, 12108–12111.
- 32 H. Zhou, M. H. Chua, H. R. Tan, T. T. Lin, B. Z. Tang and J. Xu, *ACS Appl. Nano Mater.*, 2019, **2**, 470–478.
- 33 C. Wannasiri, S. Channungkalakul, T. Bunchuay, L. Chuenchom, K. Uraisin, V. Ervithayasuporn and S. Kiatkamjornwong, *ACS Appl. Polym. Mater.*, 2020, **2**, 1244–1255.
- 34 S. Channungkalakul, V. Ervithayasuporn, P. Boonkitti, A. Phuekphong, N. Prigyai, S. Kladsomboon and S. Kiatkamjornwong, *Chem. Sci.*, 2018, **9**, 7753–7765.
- 35 J. Chen, L. Zheng, X. Ji, J. Wen, C.-L. Wang, L. Zhu, B. Sun, X. Wang and M. Zhu, *J. Phys. Chem. B*, 2022, **126**, 1334–1340.
- 36 J. Yin, Z. Zheng, J. Yang, Y. Liu, L. Cai, Q. Guo, M. Li, X. Li, T. L. Sun, G. X. Liu, C. Huang, S. Z. D. Cheng, T. P. Russell and P. Yin, *Angew. Chem. Int. Ed.*, 2021, **60**, 4894–4900.
- 37 J.-H. Zhu, S.-M. Yiu, B. Z. Tang and K. K.-W. Lo, *Inorg. Chem.*, 2021, **60**, 11672–11683.
- 38 H. Narikiyo, T. Kakuta, H. Matsuyama, M. Gon, K. Tanaka and Y. Chujo, *Bioorg. Med. Chem.*, 2017, **25**, 3431–3436.
- 39 R. Nakamura, H. Narikiyo, M. Gon, K. Tanaka and Y. Chujo, *Mater. Chem. Front.*, 2019, **3**, 2690–2695.
- 40 H. Narikiyo, M. Gon, K. Tanaka and Y. Chujo, *Mater. Chem. Front.*, 2018, **2**, 1449–1455.
- 41 Q. Yang, J. Wang, X. Chen, W. Yang, H. Pei, N. Hu, Z. Li, Y. Suo, T. Li and J. Wang, *J. Mater. Chem. A*, 2018, **6**, 2184–2192.
- 42 F. Klanberg and E. L. Muettterties, *Inorg. Chem.*, 1968, **7**, 155–160.
- 43 C. Shiau, T.-L. Hwang and C.-S. Liu, *J. Organomet. Chem.*, 1981, **214**, 31–39.
- 44 S. K. Kim, J. H. Bok, R. A. Bartsch, J. Y. Lee and J. S. Kim, *Org. Lett.*, 2005, **7**, 4839–4842.
- 45 Y. Ma, Y. Xia, Y. Zhu, F. Zhang, J. Cui, T. Jiang, X. Jia and X. Li, *RSC Adv.*, 2022, **12**, 475–482.

Supporting Information

Development of a Fluoride-Ion Sensor based on Aggregation of a Dye-modified Polyhedral Oligomeric Silsesquioxane

Daisuke Iizuka, Masayuki Gon, Kazuo Tanaka* and Yoshiki Chujo

Department of Polymer Chemistry, Graduate School of Engineering, Kyoto University Katsura, Nishikyo-ku, Kyoto 615-8510, Japan

E-mail: tanaka@poly.synchem.kyoto-u.ac.jp

Contents	page
Materials and Methods	S-3
Synthetic procedures and characterization	
Synthesis of C343-POSS	S-4
Synthesis of C343-arm	S-6
IR spectra	S-8
Optical Properties	S-8
DLS Measurement	S-10
Solvent Effect	S-10
Mass Spectrometry of Decomposition Compounds	S-11
Limit of Detection	S-12
Mechanism Study	S-13
Thermal Analysis	S-15
References	S-16

Materials and Methods

Instrumentation

^1H , ^{13}C and ^{29}Si NMR spectra were recorded on JEOL AL400 instruments at 400, 100 and 80 MHz respectively. ^{19}F NMR spectra were recorded on JEOL ECZ400S instruments at 376 MHz. Samples were analyzed in CDCl_3 . The chemical shift values were expressed relative to Me_4Si (^1H , ^{13}C and ^{29}Si) and C_6F_6 (^{19}F , -163 ppm) as internal standards in CDCl_3 . High-resolution mass (HRMS) spectrometry was performed on an EXACTIVE Plus (Thermo Fisher Scientific) at the Technical Support Office (Department of Synthetic Chemistry and Biological Chemistry, Graduate School of Engineering, Kyoto University), and the high-resolution mass spectra (HRMS) were obtained on a Thermo Fisher EXACTIVE for electrospray ionization (ESI). UV-vis spectra were recorded on a SHIMADZU UV-3600i Plus spectrophotometer, and samples were analyzed at room temperature. Fluorescence emission spectra were measured with a HORIBA JOBIN YVON Fluorolog-3 spectrofluorometer. Absolute photoluminescence quantum efficiency (Φ_{PL}) was recorded on a Hamamatsu Photonics Quantaaurus-QY Plus C13534-01. Elemental analyses were performed with a MICRO CORDER MT-5 (YANACO CO., Ltd.) at the Microanalytical Center of Kyoto University. Thermogravimetric analysis (TGA) was recorded on a Hitachi High-Tech Science Corporation. TA STA7200RV. Differential scanning calorimetry (DSC) was recorded on a Hitachi High-Tech Science Corporation. TA DSC7020. The sample on the aluminum pan was heated at the rate of 10 $^\circ\text{C}/\text{min}$ under nitrogen flowing (50 mL/min). The dynamic light scattering (DLS) measurements were carried out at 90° scattering angle and 20 ± 0.2 $^\circ\text{C}$ using a FPAR-1000 particle analyzer with a He-Ne laser as a light source. The CONTIN program was used for data analysis to extract information on the average hydrodynamic size. All reactions were performed under nitrogen atmosphere.

Materials.

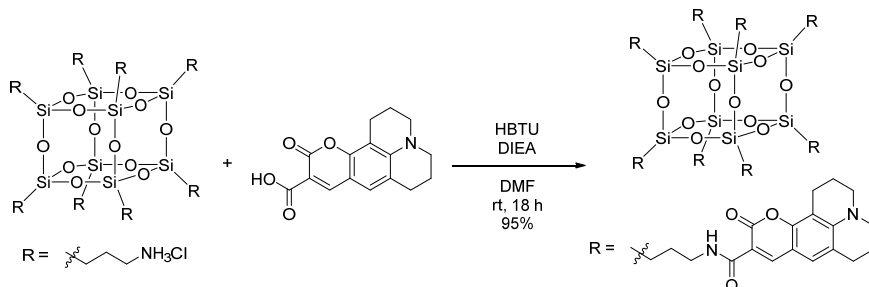
Propylamine, 4-(diethylamino)salicylaldehyde was purchased from Tokyo Chemical Industry Co, Ltd. Tetrabutylammonium fluoride (1 M in THF solution), *N,N*-diisopropylethylamine (DIEA), meldrum's acid, and 4-(4,6-dimethoxy-1,3,5-triazin-2-yl)-4-methylmorpholinium chloride (DMT-MM) were purchased from FUJIFILM Wako Pure Chemical Corporation. 1-[Bis(dimethylamino)methylene]-1*H*-benzotriazolium 3-oxide hexafluorophosphate (HBTU) was purchased from PEPTIDE INSTITUTE, INC. *N,N*-Dimethylformamide (DMF) (deoxidized grade), and dimethyl sulfoxide (DMSO) (deoxidized grade) were purchased from Wako and used as the reaction solvent. All compounds were used without purification. Octakis(3-aminopropyl) POSS hydrochloride (**Amino-POSS**)¹ and coumarin 343 (C343)² were synthesized according to the literatures.

Sample Preparation for Optical Measurements for Anion Sensing

The stock solution of **C343-POSS** in CHCl₃ (1.6×10^{-3} M per C343 unit) was prepared. This stock solution (30 μ L) was diluted with THF (2970 μ L) and stirred on a Fisher vortex for 30 s with a speed of 8 to obtain **C343-POSS** (1.6×10^{-5} M per C343 unit) in THF/CHCl₃ (99/1 v/v) mixed solution. Diluted TBAF in THF (3 μ L) was added within 30 s and stirred again for 30 s to prepare each concentration. The measurements were initiated 15 min after the end of stirring for Figures 2a and S11, and 1 min after the end of stirring for Figures 2b and 2c to monitor the difference. In the case of anti-interference tests, the anions in THF (3 μ L, 1.0×10^{-5} M) were added within 1 min.

Synthetic Procedures and Characterization

Synthesis of C343-POSS



C343 (55.3 mg, 0.19 mmol) and HBTU (88.3 mg, 0.23 mmol) were placed in a round-bottom flask equipped with a magnetic stirring bar. DMF (10 mL) and DIEA (0.081 mL, 0.47 mmol) were added to the flask. After the mixture was activated at room temperature for 30 min, Amino-POSS (22.8 mg, 0.019 mmol) was added to this solution and stirred for 18 h. The precipitate was collected by filtration, washed with DMF, cyclohexane and dried *in vacuo*. The yellow solid of **C343-POSS** (55.4 mg, 0.0183 mmol, 95%) was then obtained.

^1H NMR (CDCl_3 , 400 MHz) δ 8.81 (t, $J = 5.6$ Hz, 1H), 8.48 (s, 1H), 6.88 (s, 1H), 3.46-3.41 (m, 2H), 3.27-3.22 (m, 4H), 2.77 (t, $J = 6.3$ Hz, 2H), 2.69 (t, $J = 6.2$ Hz, 2H), 1.91 (d, $J = 5.1$ Hz, 4H), 1.77-1.72 (m, 2H), 0.75-0.71 (m, 2H) ppm; ^{13}C NMR (CDCl_3 , 100 MHz) δ 163.3, 162.7, 152.3, 147.7, 147.5, 126.8, 119.2, 109.2, 108.1, 105.4, 50.1, 49.7, 42.1, 27.3, 23.0, 21.1, 20.1, 20.0, 9.4 ppm; ^{29}Si NMR (CDCl_3 , 80 MHz) δ -66.9 (s) ppm. HRMS (ESI) calcd. for $\text{C}_{152}\text{H}_{168}\text{N}_{16}\text{O}_{32}\text{Si}_8$ $[\text{M}+\text{Na}]^+$: 3039.9853, found: 3039.9855.

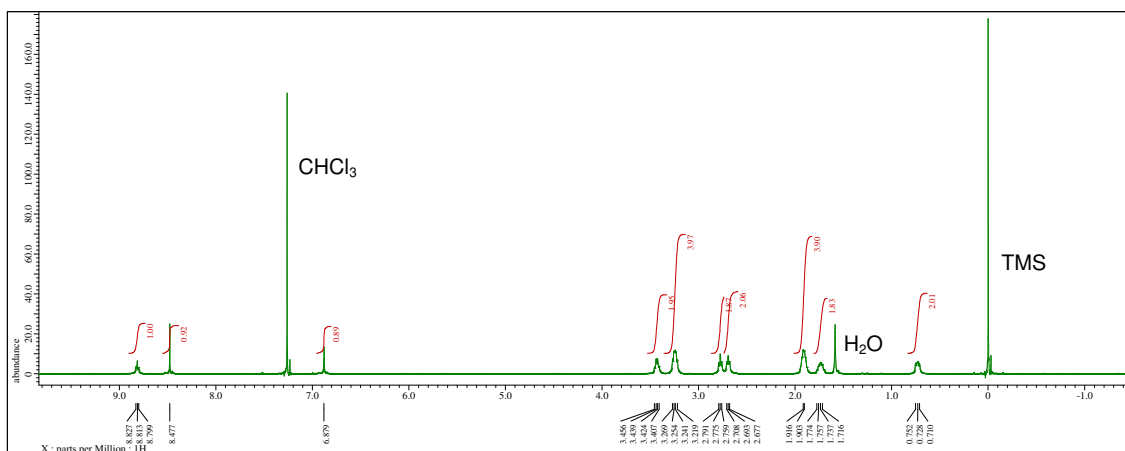


Figure S1. ^1H NMR spectrum of **C343-POSS** in CDCl_3 .

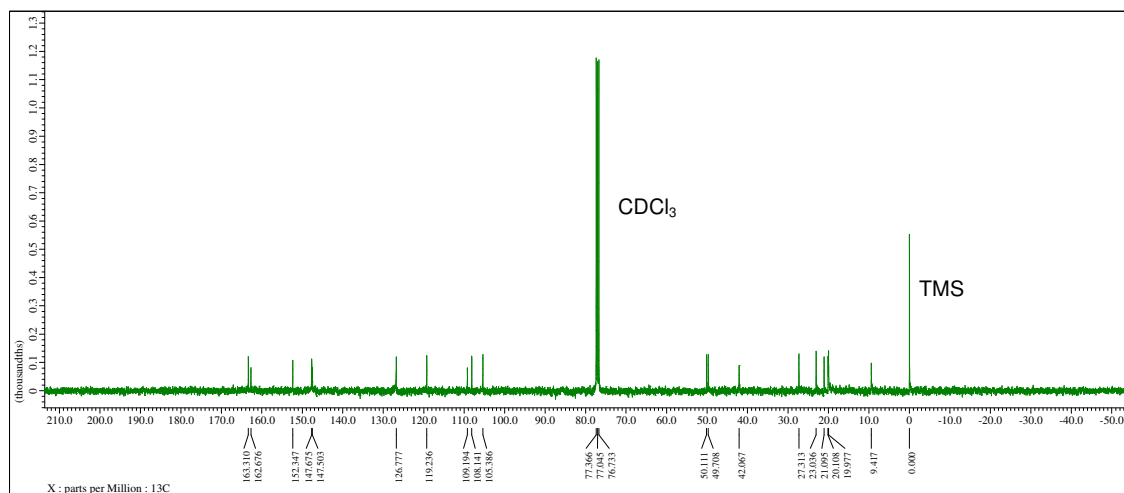


Figure S2. ^{13}C NMR spectrum of C343-POSS in CDCl_3 .

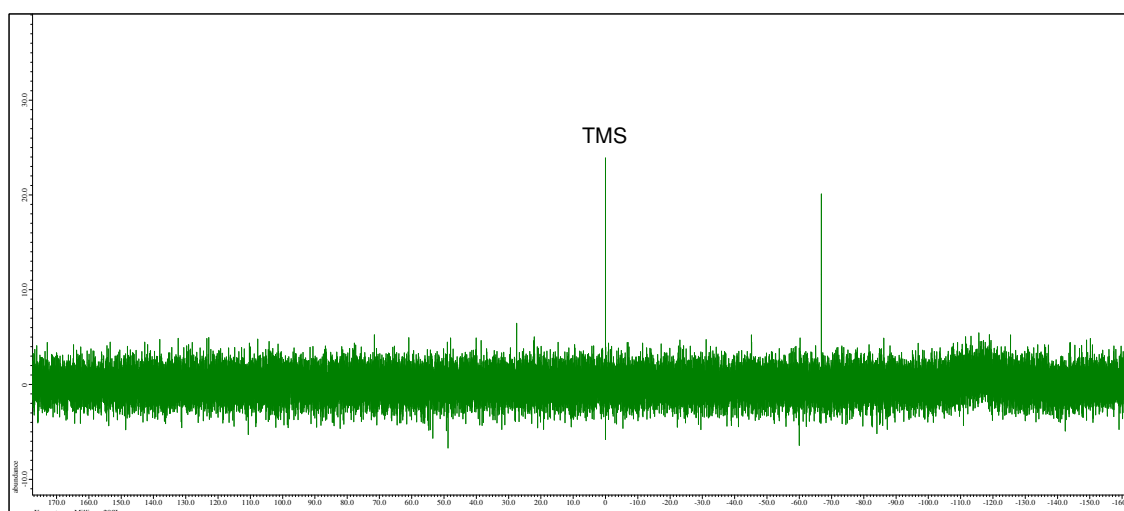
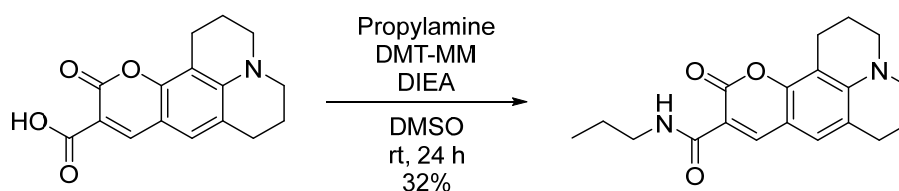


Figure S3. ^{29}Si NMR spectrum of C343-POSS in CDCl_3 .

Synthesis of C343-arm



C-343 (28.5 mg, 0.1 mmol) was dissolved in 5 mL of DMSO in a flask. DMT-MM (55.3 mg, 0.2 mmol) was added to the solution, and the mixture was stirred at room temperature for 30 min, followed by addition of propylamine (5.9 mg, 0.1 mmol) and DIEA (34.8 μL , 0.2 mmol). The mixture was

additionally stirred at room temperature for 24 h and dropped into 250 mL of 0.5 M NaHCO₃ aq. and the products were precipitated. The precipitation was collected by filtration and washed with water and dried *in vacuo*. Recrystallization from hot EtOH/water afforded **C343-arm** as a yellow crystal (10.6 mg, 0.032 mmol, 32%).

¹H NMR (CDCl₃, 400 MHz) δ 8.87 (s, 1H), 8.61 (s, 1H), 7.01 (s, 1H), 3.40 (d, *J* = 5.9 Hz, 2H), 3.33 (s, 4H), 2.89 (t, *J* = 6.4 Hz, 2H), 2.78 (t, *J* = 6.6 Hz, 2H), 1.98-1.98 (m, 4H), 1.65-1.63 (m, 2H), 0.98 (t, *J* = 6.9 Hz, 3H) ppm; ¹³C NMR (CDCl₃, 100 MHz) δ 163.5, 163.1, 152.6, 148.0, 148.0, 127.0, 119.6, 109.3, 108.3, 105.7, 50.2, 49.8, 41.3, 27.5, 22.9, 21.2, 20.2, 20.1, 11.5 ppm. HRMS (ESI) calcd. for C₁₉H₂₀N₂O₃ [M+Na]⁺: 349.1523, found: 349.1527.

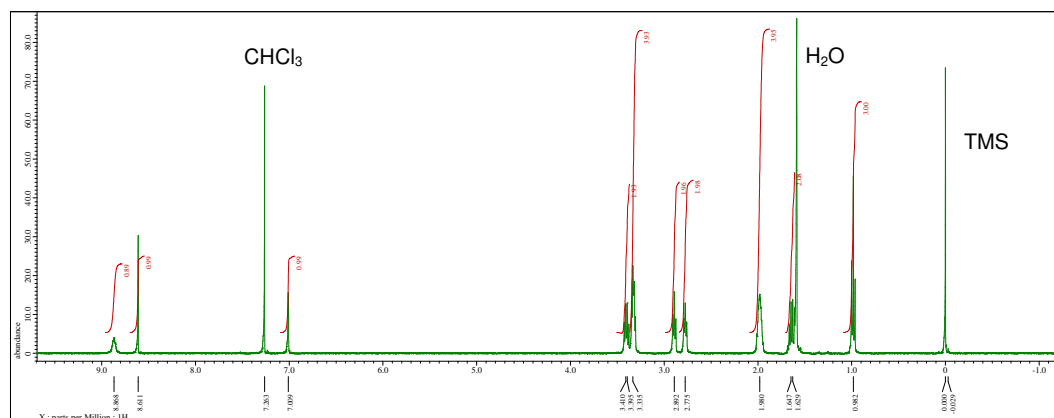


Figure S4. ¹H NMR spectrum of **C343-arm** in CDCl₃.

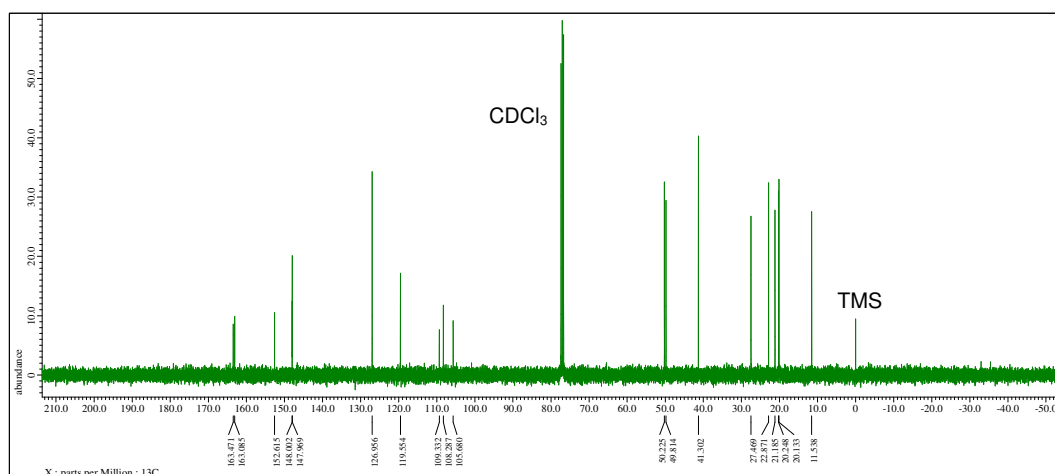


Figure S5. ¹³C NMR spectrum of **C343-arm** in CDCl₃.

IR Spectra

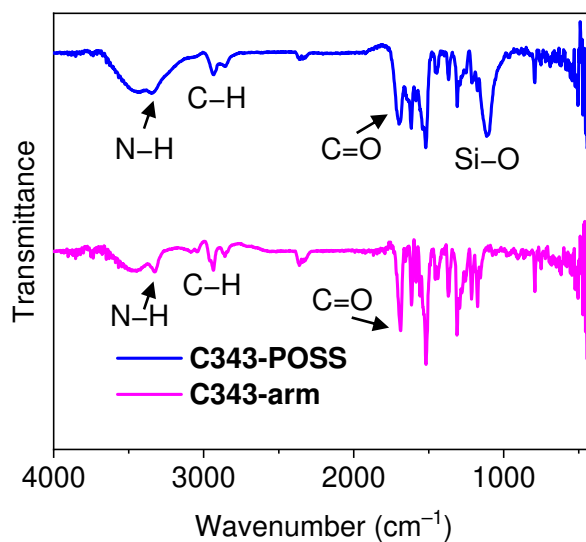


Figure S6. IR spectra of **C343-POSS** and **C343-arm** in KBr pellets.

Optical Properties

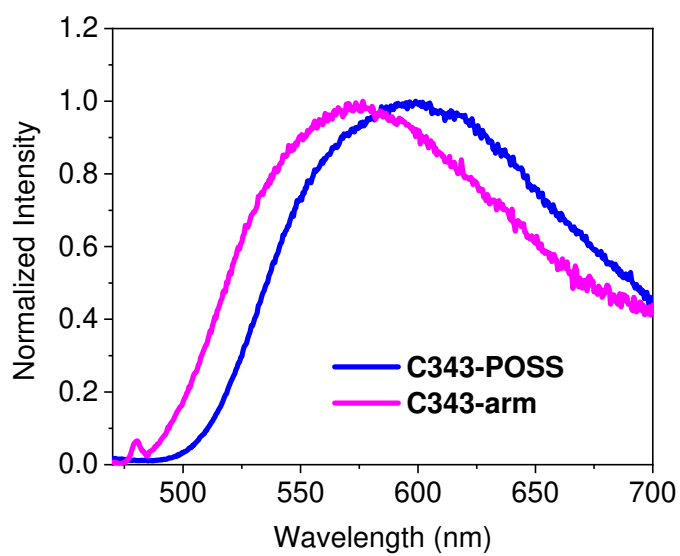


Figure S7. Emission spectra of **C343-POSS** and **C343-arm** in the solid state.

Table S1. Optical data of C343-POSS and C343-arm in solution and solid states

		$\lambda_{\max}^{\text{abs}}$ (nm)	$\lambda_{\max}^{\text{em}}$ (nm) ^c	$\epsilon(\text{M}^{-1} \text{cm}^{-1})^d$	Φ_{PL} (%)
C343-POSS	CHCl_3 ^a	429	461	37,300	30
	THF/ CHCl_3 ^b	418	464, 541	20,100	9
	solid	-	596	-	2
C343-arm	CHCl_3 ^a	432	460	48,000	85
	THF/ CHCl_3 ^b	425	462	43,700	82
	solid	-	574	-	5

^a 1.6×10^{-5} M per C343 unit (absorption), 8.0×10^{-6} M per C343 unit (emission and Φ_{PL}).

^b In THF/ CHCl_3 = 99/1 v/v mixed solution, 1.6×10^{-5} M per C343 unit.

^c Excited at the wavelengths of absorption maxima (λ_{abs}).

^d Calculated based on the concentration of C343 unit.

DLS Measurement

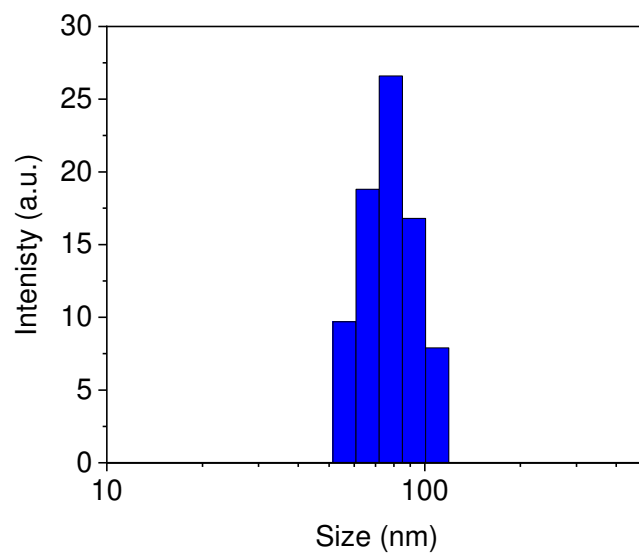


Figure S8. Number-averaged hydrodynamic size distribution of **C343-POSS** (1.6×10^{-5} M per C343 unit) in the THF/ CHCl_3 (99/1 v/v) mixed solution.

Solvent Effect

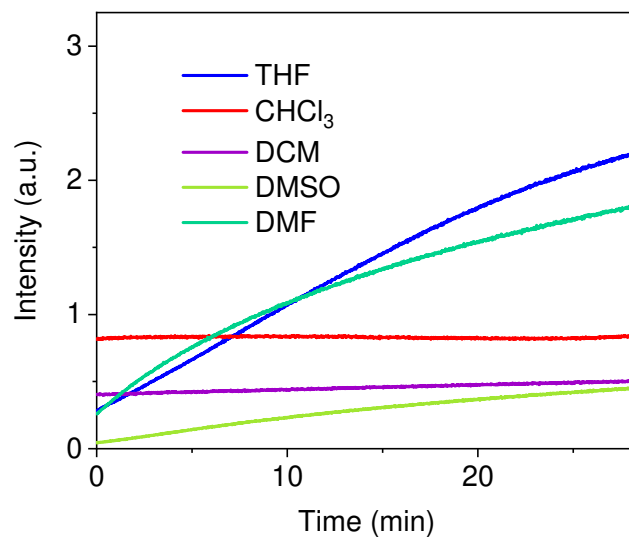


Figure S9. Photoluminescence intensity kinetics of **C343-POSS** (1.6×10^{-5} M per C343 unit) in various solutions (solvent/ $\text{CHCl}_3 = 99/1$ v/v) upon the addition of TBAF (100 equiv.).

Limit of Detection

The calculation of the limit of detection (L_D) was carried out by the data from 0 to 20 μM of TBAF with good correlation between fluoride concentration and fluorescence intensity at low concentration area. This is because at high concentration such as 50 μM (25 equiv. or 3.125 equiv. per C343 unit), fluoride anions should be overconsumed and L_D might be underestimated.

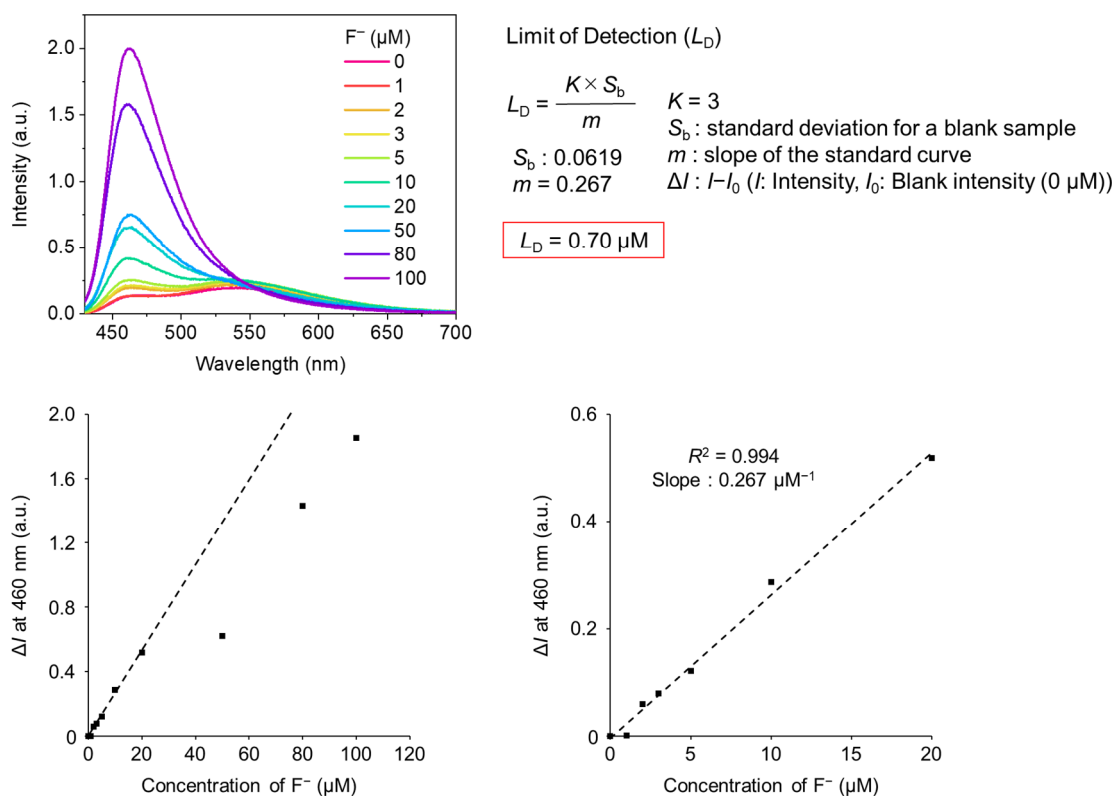
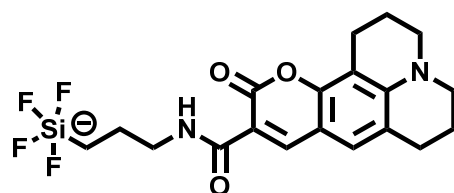


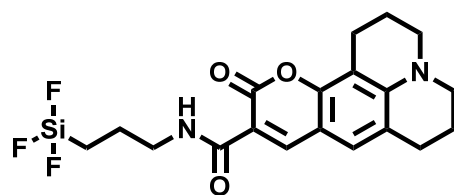
Figure S10. Fluorescence enhancement upon addition of F^- and calculation of limit of detection (L_D). $[\text{C343-POSS}] = 1.6 \times 10^{-5} \text{ M}$ per C343 unit in THF/ CHCl_3 (99/1 v/v) mixed solution. The cation is tetrabutylammonium (TBA).

Mass Spectrometry of Decomposition Compounds



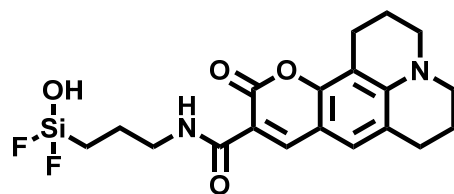
D1

HRMS (ESI) calcd. for $C_{19}H_{21}F_4N_2O_3Si$ $[M-H]^-$: 429.1263 found: 429.1262



D2

HRMS (ESI) calcd. for $C_{19}H_{21}F_3N_2O_3Si$ $[M-H]^-$: 409.1201 found: 409.1200



D3

HRMS (ESI) calcd. for $C_{19}H_{22}F_2N_2O_4Si$ $[M-H]^-$: 407.1244 found: 407.1245

Figure S11. Molecular weights obtained from HRMS spectra of decomposition products.

Mechanism Study

TBAF only

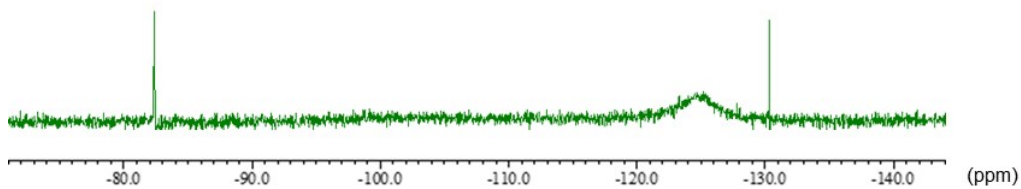


Figure S12. ^{19}F NMR spectrum of TBAF in CDCl_3 after 12 h of standstill at room temperature.

C343-POSS

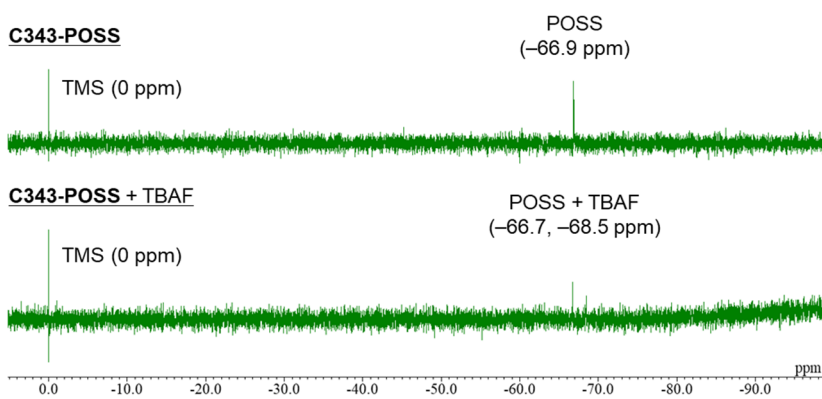


Figure S13. ^{29}Si NMR of C343-POSS before and after the addition of TBAF in CDCl_3 .

C343-POSS

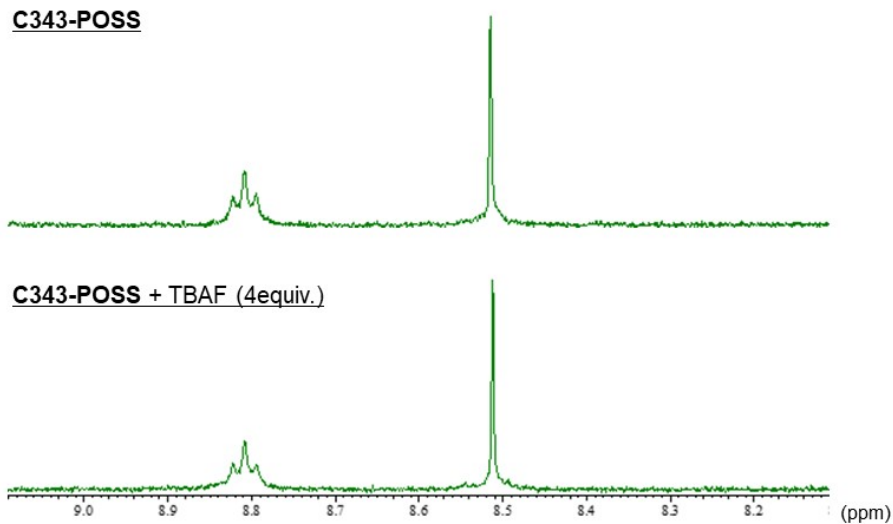
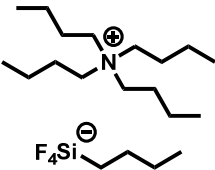
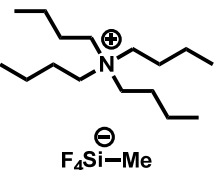
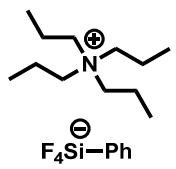
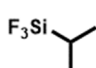



Figure S14. ^1H NMR of C343-POSS before and after the addition of TBAF (4 equiv.) in CDCl_3 . The peak of δ 8.81 ppm is attributed to amide proton.

Table S2. ^{19}F NMR data in previous reports

Compound	Solvent	Chemical shift (ppm)	reference
	CD_2Cl_2	-116.6	[3]
	CD_2Cl_2	-110.5	[3]
	CDCl_3	-119.2	[4]
	CDCl_3	-142.2	[4]
	CDCl_3	-137.98	[4]

Thermal analysis

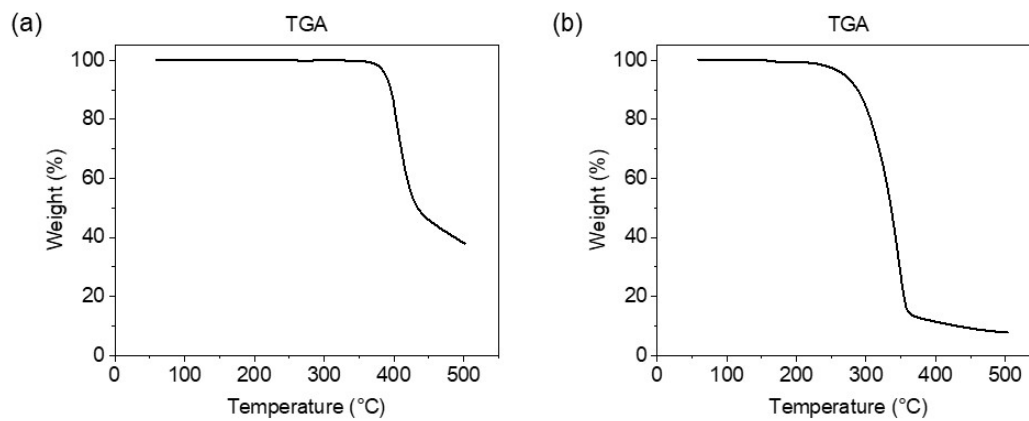


Figure S15. TGA curves of (a) C343-POSS and (b) C343-arm.

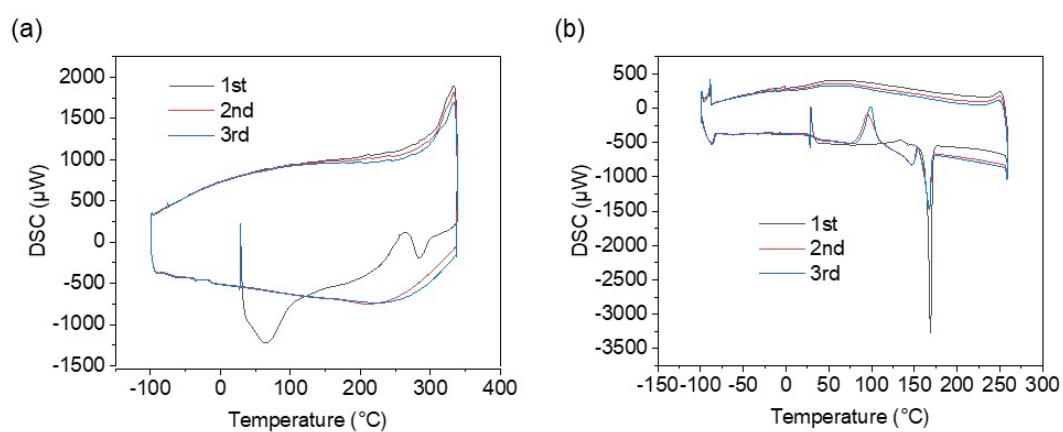


Figure S16. DSC thermograms of (a) C343-POSS and (b) C343-arm.

References

1. K. Tanaka, K. Inafuku, S. Adachi and Y. Chujo, *Macromolecules*, 2009, **42**, 3489–3492.
2. N. Draoui, O. Schicke, A. Fernandes, X. Drozak, F. Nahra, A. Dumont, J. Douxfils, E. Hermans, J.-M. Dogné, R. Corbau, A. Marchand, P. Chaltin, P. Sonveaux, O. Feron and O. Riant, *Bioorg. Med. Chem.*, 2013, **21**, 7107–7117.
3. F. Klanberg, and E. L. Muetterties, *Inorg. Chem.*, 1968, **7**, 155–160.
4. C. Shiau, T.-L. Hwang and C.-S. Liu, *J. Organomet. Chem.*, 1981, **214**, 31–39.